Proceedings of the 5th IEEE International Workshop on Metrology for AeroSpace (MetroAeroSpace),
20-22 June 2018, Rome, Italy. pp. 56-61
DOI:10.1109/MetroAeroSpace.2018.8453598

Inspection of Aircraft Wing Panels Using Unmanned Aerial Vehicles

Konstantinos Malandrakis, Al Savvaris, Jose Angel Gonzalez Domingo, Nick Avdelidis,
Panagiotis Tsilivis, Florence Plumacker, Luca Zanotti Fragonara, Antonios Tsourdos
Centre for Autonomous and Cyber-Physical Systems
Cranfield University
Cranfield, UK
k.malandrakis@cranfield.ac.uk

***Abstract*—In large civil aircraft manufacturing a time-consuming post-production process is the non-destructive inspection of wing panels. This work aims to address this challenge and improve the defects' detection by performing automated aerial inspection using a small off-the-shelf multirotor. The UAV is equipped with a wide field-of-view camera and an ultraviolet torch for implementing non-invasive imaging inspection. In particular, the UAV is programmed to perform the complete mission and stream video, in real-time, to the ground control station where the defects' detection algorithm is executed. The proposed platform was mathematically modelled in MATLAB/SIMULINK in order to assess the behaviour of the system using a path following method during the aircraft wing inspection. The UAV was tested in the lab where a six-meter-long wing panel was one-side inspected. Initial results indicate that this inspection method could reduce significantly the inspection time, cost, and workload, whilst potentially increasing the probability of detection.**

***Index Terms*—Non-Destructive Testing, Ultraviolet light, Automated inspection, Defects detection, UAV**

I. Introduction

Over the last few years, the number of air passengers carried worldwide has increased by 63.1% [1]. In many forecasts, [2], [3] is depicted that in the next twenty years the world annual passenger and cargo air traffic is expected to have an upward trend with an approximately annual growth rate at 4.5%. At the same time, the post-production and maintenance Non-Destructive Inspection (NDI) or Non-Destructive Testing (NDT) on aircraft is anticipated to be in high workload levels. Motivated by this, global players from commercial aircraft industry design new production lines to accelerate the inspection process by utilising automated systems for heating, cleaning, chemical applications, and so forth. However, some inspection tasks are still carried out by a human operator. As a result, this might slow down the inspection chain. A promising solution for this challenge is the utilisation of automated systems, as proposed in [4], where an automated non-contact laser ultrasonic technology has the potential to increase the annual revenue by up to 26.3% and crack detection rates from 44% to 95% during the inspection.

Recently, Unmanned Aerial Vehicles (UAVs) have attracted significant attention, for both military and civil applications, due to the advancements in processing power, miniaturisation of sensors and components that have led to an increase in the number of areas where they can be deployed. More precisely, a UAV could perform missions, such as search & rescue, disaster relief, surveillance, surveying, and so forth. Several researchers [5]–[10], have proposed the use of small UAVs for monitoring and inspection of infrastructures, such as buildings, wind turbines, photovoltaic systems, power transmission lines, and gas pipelines. More precisely, the employment of UAVs for aerial inspection could minimise the risk of height hazard, inspection time, and cost, since large areas under inspection are mainly assessed, in real-time, by minimum human interventions and without the utilisation of any special infrastructure [5], [7], [9]–[13].

Taking into consideration the aforementioned benefits of the aerial inspections, this work assesses the significance of using a UAV on accelerating and improving the aircraft's wing panel inspection. Although research has been carried out on automated aerial inspection and maintenance on aircraft parts by using UAVs, no studies have been reported. The majority of the published papers, in this field, implement autonomous ground vehicles [14] or robotic arms for defects detection. However, those autonomous systems might not be suitable for all the applications, because ground vehicles might not inspect high facilities, whilst robotic arms might require expensive equipment and appropriate infrastructure.

The main purpose of the NDT is to define the airworthiness

Fig. 1. The aerial vehicle used in the proposed inspection methods.

(a) The concept of using the onboard UV-light for flow penetrant testing.

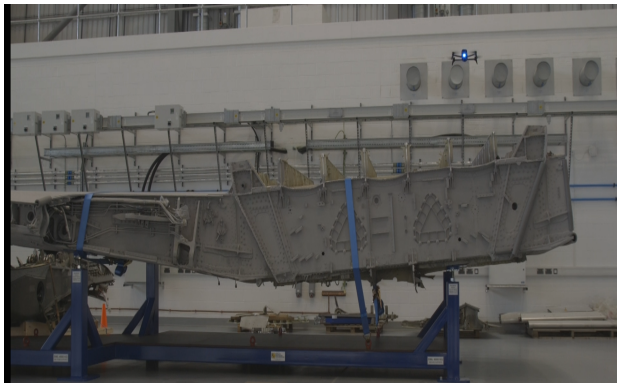

(b) Aerial visual inspection of the top aspect of a wing.

Fig. 2. Aerial inspection.

of a component without damaging it. In general, several NDT methods are available, such as those mentioned in [15], [16], include techniques such as visual, borescope, liquid penetrant, Eddy current, ultrasonic, acoustic emission, magnetic particle, and radiographic. Among these NDT methods, this study focuses on the visual and liquid penetrant inspection of wing panels by performing preprogrammed missions with a small quadrotor that is illustrated in Fig. 1. The work presented in this paper covers the development of the complete system for aerial wing inspection, includes the developed path following algorithm and the defect detection algorithm, and assesses their performance.

The paper is organised into six sections. In the following section, the selected aerial platform and experimental setup are presented. The third section describes the applied path following method for the aerial wing inspection in a simulation environment. In the fourth section, the developed image processing method for the defects' detection is analysed, while the scenario of the performed non-destructive testing is presented. Section five assesses the obtained results from the inspection and the fidelity of the system. In the last section, the significance of the findings is outlined, while further work on this study is recommended.

II. Hardware Selection and Experimental Setup

In this section, the subsystems and architecture of the experimental setup are described. The setup mainly consists of the aerial vehicle, the Ground Control Station (GCS), and the wing panel for inspection.

In this work, the commercially available Bebop 2 Power, from Parrot, was chosen as the platform for performing the aerial inspection of the wing panels. This quadrotor is $0.3\,\mathrm{m}$ in diameter and weighs $0.52\,\mathrm{kg}$, whilst is capable to perform missions in both indoor and outdoor environments. This version of Bebop 2 has an upgraded battery capacity that extends the flight time to $30\,\mathrm{min}$. However, the UAV has a reduced flight endurance of approximate $17\,\mathrm{min}$, due to the extra payload of the UV-light. The onboard platform sensors ensure accurate positioning and control of the air vehicle. More precisely, the UAV is equipped with an IMU, a GPS, a downward camera, and an ultrasonic sensor for defining the attitude and position of the vehicle. The platform is equipped with an 8 GB internal flash memory that is sufficient for recording long-duration videos. Furthermore, is equipped with 14-megapixel CMOS wide-angle camera with digital image stabilisation that can capture full high-definition at 1080p and 30fps video. It is worth noting that the custom-made wide-angle lens and the advanced anti-distortion system of the onboard camera allow the UAV to perform visual inspection above or below the wing as is presented in Fig. 2a. This module is important for both tested inspection methods. Another critical component of the air vehicle is the Wi-Fi module that is utilised for receiving commands and live streaming images and video to a mobile/tablet or in this project to the GCS.

Last but not least, Bebop 2 is compatible with other instruments such as FLIR ONE Pro camera that can be used for thermal inspection.

In order to perform the penetrant flow detection, a UV light that fulfils the following requirements is needed:

- The wavelength range of the UV light has to be between $315\,\mathrm{nm}$ to $400\,\mathrm{nm}$ with a peak at $365 \pm 5\,\mathrm{nm}$.
- The intensity at examination surface has to be between $12\,\mathrm{W\,m^{-2}}$ and $50\,\mathrm{W\,m^{-2}}$.
- The battery has to be rechargeable.
- Have as minimum size and weight as possible.

Considering the aforementioned requirements, the UGV3 UV LED torch, from Labino, was chosen and mounted on the proposed UAV as is illustrated in Fig. 1. The UV light is $0.159\,\mathrm{m}$ long, weighs $0.21\,\mathrm{kg}$ and provides the right illumination levels for the inspection. More precisely, at a distance of $1\,\mathrm{m}$ from the panel, the torch emits a mid-light beam with an approximate intensity of $18\,\mathrm{W\,m^{-2}}$. Using trigonometry, the diameter of lighting can be deduced about $0.26\,\mathrm{m}$.

The aerial platform connects wirelessly to the GCS for transmitting, in real-time, video of the inspection and receiving flight commands. The GCS is a workstation with a wireless USB module. The primary objective of this subsystem is to execute the algorithms in order to detect, display, classify and

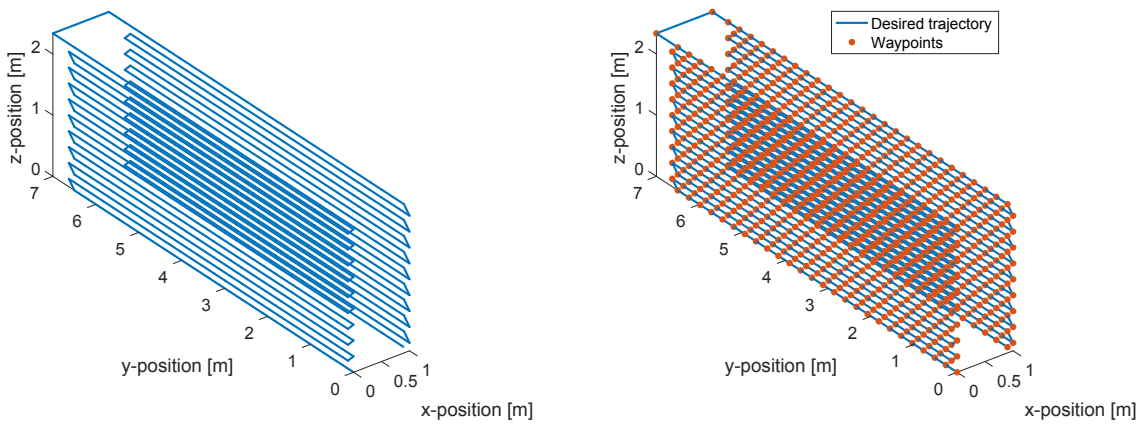

Fig. 3. Desired waypoints and trajectory used for the simulations.

log defects from the inspection. Another important objective is to send flight commands to the aerial platform.

In this work, a wing panel was utilised to examine the fidelity of the proposed aerial NDT methods. A $6\,\mathrm{m}$ long wing panel was vertically mounted to perform the visual and flow penetrant inspection methods, as shown in Fig. 2a. However, an example of a complete wing, from an Airbus 320, is also presented in Fig. 2b in order to illustrate the applicability of the proposed concept in horizontally installed wings.

III. Path Following Method

The proposed platform was designed and mathematically modelled in MATLAB/SIMULINK in order to assess the behaviour and performance of the quadrotor using a path following method during the aircraft wing inspection.

In this study, different types of path following algorithms, such as carrot-chasing, non-linear guidance law (NLGL), pure pursuit and LOS-based, vector field-based, and LQR, could be considered. However, the NLGL was chosen and examined because is an easy-to-implement algorithm and robust against wind disturbances [17].

Fig. 3 presents the waypoints and trajectory that need to be followed in the simulation of a two-sided inspection. The total inspection time for two-side wing panel was estimated at $1200\,\mathrm{s}$, for a total approximately flight distance of $252\,\mathrm{m}$. The velocity of the vehicle is considered constant. In the simulation model, a wing panel with $6.5\,\mathrm{m}$ span, $2.33\,\mathrm{m}$ chord, and $0.3\,\mathrm{m}$ thickness, is considered. The wing panel is assumed as a rectangular surface for simplifying its design complexity. The proposed inspection method is based on the full coverage of the rectangle with UV lighting disks, as is shown in Fig. 4. The UAV keeps $1\,\mathrm{m}$ separation distance from the wing panel (x-axis) and hence the UV lighting diameter, which expresses the disks, is about $0.26\,\mathrm{m}$. In the simulated mission, the UAV follows waypoints that have separation distance (D) $0.26\,\mathrm{m}$ along y-axis, $0.13\,\mathrm{m}$ in z-axis, as is shown in Fig. 4a. An example of a wing panel that is completely covered by UV lighting disks as is illustrated in Fig. 4b. In this example, the number of waypoints for one-side inspection is set at 494 waypoints.

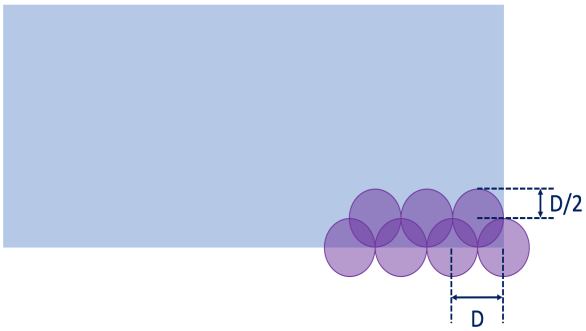

(a) Waypoints' separation distance along y-axis and z-axis.

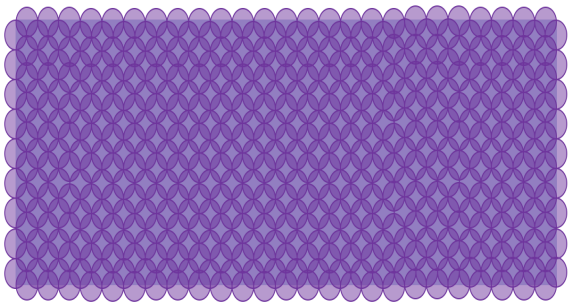

(b) Full coverage of the rectangle with UV lighting disks.

Fig. 4. NDT simulated inspection.

IV. Non-Destructive Testing

Currently, the time length required for the penetrant flow detection process, when performed by one technician, varies with respect to the surface length; from $1\,\mathrm{h}$ to $4\,\mathrm{h}$. The aerial inspection was designed and developed in order to further reduce the cost and the time of this process. The UAV captures high-quality video and transmits it, in real-time, to the workstation, while simultaneously it is been saved in the internal memory. The GCS receives the video frames and executes the image processing algorithms to detect and classify defects.

A. Image processing algorithm

The image processing algorithm was developed in Python/OpenCV. In the source code, the frame passes from different processing stages in order to give the desired outcome. An example of the image processing sequence is given in Fig. 5, where the implemented image processing algorithm output is shown. More specifically, Fig. 5a illustrates the captured image under UV light. Next, Fig. 5b presents the gamma corrected image, where only the defects are highlighted. Additional filters were also applied to reduce the noise and other false positives in the image. The Canny edge detector follows in the script and prepares the image with the detected defects for classification. Following that, the developed code estimates the relative size and metric position of the defects on the image, as is illustrated in the Fig. 5c. It is worth mentioning that, at the end of the mission, the number of the detected defects are calculated and displayed. In the example of Fig. 5, the algorithm detected 114 defects with size from $2.54\,\mathrm{mm}$ to $12.7\,\mathrm{mm}$.

B. Inspection Scenario

Another function of the workstation is to define the mission plan of the aerial platform according to the object dimensions and NDT method. The experimental inspection follows a similar procedure to the simulated with the difference that no path following method is applied. In addition, the mission used as a test case here is of one-side inspection of the six-meter long wing panel. This scenario contains 18 waypoints with $1\,\mathrm{m}$ separation distance, in y-axis and $0.5\,\mathrm{m}$ in z-axis, as illustrated in Fig. 6. The UAV starts its mission with an autonomous take-off (green arrow) and ends in the last waypoint with an autonomous landing (blue arrow). The overall mission lasts $118\,\mathrm{s}$, where at each waypoint the UAV hovers for $6\,\mathrm{s}$.

For the inspection, the workstation sends a predefined position coordinates to the UAV. In the visual inspection, the vehicle follows the mission scenario by using the downward camera and the ultrasonic sensor. In the flow penetrant inspection, an external positioning system such as VICON system or a Real-Time Location System (RTLS) is required to support the guidance law of the UAV since the dark environment does not allow the optic flow algorithm to work properly. In this experiment, the penetrant was applied only in the area marked by the green rectangular as shown in Fig. 6.

(a) Raw captured image.

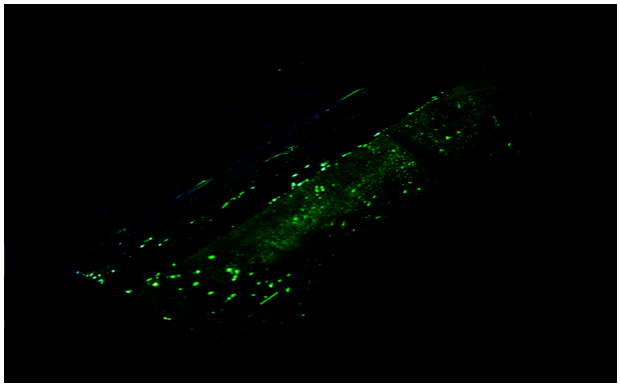

(b) Filtered image.

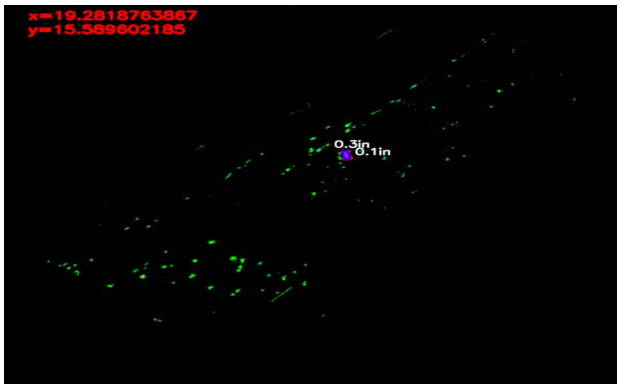

(c) Size and position of detected defects on image.

Fig. 5. Sequence of image processing method.

V. Results and Discussion

Simulation results indicate that the NLGL provides satisfactory performance. More precisely, the complete inspection of a whole panel, using NLGL, lasted $1260\,\mathrm{s}$ that corresponds to less than 5% discrepancy from the estimated.

The results of the actual aerial inspections indicated that the UAV can carry out successfully both visual and flow penetrant inspections. In visual inspection, the aerial vehicle was robust and stable using the optic flow algorithm. The UAV could land with an uncertainty up to $\pm 0.15\mathrm{m}$, in x-axis and y-axis, from the defined landing point. It was observed that

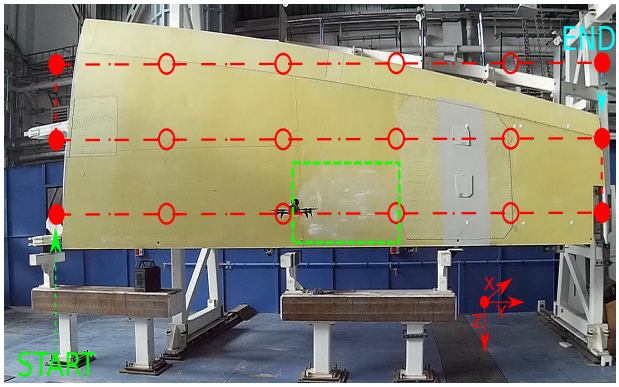

Fig. 6. Automated aerial wing inspection using 18 waypoints.

the ambient light of the inspection room significantly affected the performance of the optic flow algorithm and hence the vehicle's behaviour and performance.

The GCS was able to receive, display, process and log the streamed video from the UAV. However, it was noticed that few frames were lost during the transmission. A possible explanation for this might be the chosen video settings, such as the video codec and quality. Another possible explanation might be the computational load of the workstation since it has to read, process, display, and save videos (raw and processed) in parallel. However, for the highest fidelity and robustness, a post-processing inspection is recommended using the same algorithm with the video file that is saved in vehicle's memory.

Consequently, the automated inspection method proposed in this study permits the operator to focus on the results of raw and processed videos, without concerning with flight skills, training, regulations, and safety. It is worth mentioning that the operator with a press of the button could start the mission or terminate it by performing an autonomous landing. The implemented NDT method is designed to be GPS-independent and perform indoor inspection based-on onboard sensors.

VI. Conclusions

This study contributes to reducing the risk, time, and cost of the NDT by performing an automated aerial inspection. This research shows that the integration of a commercially available UAV equipped with a UV torch provides an easy-to-implement and robust method for visual and flow penetrant inspection. Simulation tests, in which the NLGL is applied on the modelled UAV, confirm reasonable tracking performance for the aerial wing inspection. Furthermore, experimental results show that the proposed components and architecture can offer additional capabilities to the operator such as automated record-keeping. Moreover, the results of this investigation reveal that the performance of the proposed image processing method can successfully detect defects even in a size of $2.54\,\mathrm{mm}$. Although the designed system is for real-time image processing, findings identify that a post-processing can provide more reliable results but with an approximate time penalty of $2\,\mathrm{min}$.

In the future, the fidelity and performance of the image processing algorithm would be further evaluated and validated by a qualified NDT inspector. In this manner, the probability of detection could be accurately determined. Additional work needs to be done on the computer vision algorithm in the area of the automatic defects classification based on their type, size, and significance. Moreover, the development of a graphic user interface, which would display a 3-D model of the inspected object with all detected defects projected on it, is scheduled for future work. More path following methods will be studied for determining the most appropriate guidance law for aerial inspection. Further experimental aerial inspections will be carried out including the studied path following method to validate the behaviour and performance of the simulation model.

References

[1] Eurostat. The EU in the world - transport. [Online]. Available: http://ec.europa.eu/eurostat/statistics-explained/index.php/The_EU_in_the_world_-_transport

[2] AIRBUS. Global Market Forecast 2017-2036. [Online]. Available: http://www.airbus.com/content/dam/corporate-topics/publications/backgrounders/Airbus_Global_Market_Forecast_2017-2036_Growing_Horizons_full_book.pdf

[3] Statista. Air traffic - passenger growth rates forecast 2017-2036. [Online]. Available: https://www.statista.com/statistics/269919/growth-rates-for-passenger-and-cargo-air-traffic/

[4] R. F. Fernandez, K. Keller, and J. Robins, "Design of a system for aircraft fuselage inspection," in *2016 IEEE Systems and Information Engineering Design Symposium (SIEDS)*, pp. 283–288. [Online]. Available: http://ieeexplore.ieee.org/document/7489315/

[5] P. Addabbo, A. Angrisano, M. L. Bernardi, G. Gagliarde, A. Mennella, M. Nisi, and S. Ullo, "A UAV infrared measurement approach for defect detection in photovoltaic plants," in *2017 IEEE International Workshop on Metrology for AeroSpace (MetroAeroSpace)*, pp. 345–350. [Online]. Available: http://ieeexplore.ieee.org/document/7999594/

[6] K. Malandrakis, R. Dixon, A. Savvaris, and A. Tsourdos, "Design and development of a novel spherical UAV," vol. 49, no. 17, pp. 320–325. [Online]. Available: http://www.sciencedirect.com/science/article/pii/S2405896316315270

[7] M. Aghaei, A. Dolara, S. Leva, and F. Grimaccia, "Image resolution and defects detection in pv inspection by unmanned technologies," in *2016 IEEE Power and Energy Society General Meeting (PESGM)*, July 2016, pp. 1–5.

[8] G. Morgenthal and N. Hallermann, "Quality assessment of unmanned aerial vehicle (UAV) based visual inspection of structures," vol. 17, no. 3, pp. 289–302. [Online]. Available: https://doi.org/10.1260/1369-4332.17.3.289

[9] O. McAree, J. M. Aitken, and S. M. Veres, "A model based design framework for safety verification of a semi-autonomous inspection drone," in *2016 UKACC 11th International Conference on Control (CONTROL)*, pp. 1–6. [Online]. Available: http://ieeexplore.ieee.org/document/7737551/

[10] G. Morgenthal and N. Hallermann, "Quality assessment of unmanned aerial vehicle (UAV) based visual inspection of structures," vol. 17, no. 3, pp. 289–302. [Online]. Available: https://doi.org/10.1260/1369-4332.17.3.289

[11] C. Eschmann, C.-M. Kuo, C.-H. Kuo, and C. Boller, "High-resolution multisensor infrastructure inspection with unmanned aircraft systems," *ISPRS - International Archives of the Photogrammetry, Remote Sensing and Spatial Information Sciences*, vol. XL-1/W2, pp. 125–129, 2013. [Online]. Available: https://www.int-arch-photogramm-remote-sens-spatial-inf-sci.net/XL-1-W2/125/2013/

[12] J. Nikolic, M. Burri, J. Rehder, S. Leutenegger, C. Huerzeler, and R. Siegwart, "A UAV system for inspection of industrial facilities," in *2013 IEEE Aerospace Conference*, pp. 1–8. [Online]. Available: http://ieeexplore.ieee.org/document/6496959/

[13] P. B. Quater, F. Grimaccia, S. Leva, M. Mussetta, and M. Aghaei, "Light unmanned aerial vehicles (UAVs) for cooperative inspection of PV plants," vol. 4, no. 4, pp. 1107–1113. [Online]. Available: http://ieeexplore.ieee.org/document/6828739/

[14] J. R. Leiva, T. Villemot, G. Dangoumeau, M. A. Bauda, and S. Larnier, "Automatic visual detection and verification of exterior aircraft elements," in *2017 IEEE International Workshop of Electronics, Control, Measurement, Signals and their Application to Mechatronics (ECMSM)*, pp. 1–5. [Online]. Available: http://ieeexplore.ieee.org/document/7945885/

[15] N. Montinaro, D. Cerniglia, and G. Pitarresi, "Flying laser spot thermography for the inspection of aerospace grade fibre metal laminates," in *2017 IEEE International Workshop on Metrology for AeroSpace (MetroAeroSpace)*, pp. 206–210. [Online]. Available: http://ieeexplore.ieee.org/document/7999565/

[16] Federal Aviation Administration. Aviation Maintenance Technician Handbook - General. [Online]. Available: https://www.faa.gov/regulations_policies/handbooks_manuals/aircraft/amt_handbook/

[17] P. B. Sujit, S. Saripalli, and J. B. Sousa, "Unmanned aerial vehicle path following: A survey and analysis of algorithms for fixed-wing unmanned aerial vehicless," *IEEE Control Systems*, vol. 34, no. 1, pp. 42–59, Feb 2014. [Online]. Available: https://ieeexplore.ieee.org/stamp/stamp.jsp?tp=&arnumber=6712082